

An Integrated Approach to Produce Robust Deep Neural Network Models with High Efficiency

Zhijian Li , Bao Wang, and Jack Xin

Abstract—Deep Neural Networks (DNNs) needs to be both efficient and robust for practical uses. Quantization and structure simplification are promising ways to adapt DNNs to mobile devices, and adversarial training is one of the most successful methods to train robust DNNs. In this work, we aim to realize both advantages by applying a convergent relaxation quantization algorithm, i.e., Binary-Relax (BR), to an adversarially trained robust model, i.e. the ResNets Ensemble via Feynman-Kac Formalism (EnResNet). We discover that high precision, such as ternary (tnn) or (4-bit) quantization, produces sparse DNNs. However, this sparsity is unstructured under adversarial training. To solve the problems that adversarial training jeopardizes DNNs' accuracy on clean images and break the structure of sparsity, we design a trade-off loss function that helps DNNs preserve natural accuracy and improve channel sparsity. With our newly designed trade-off loss function, we achieve both goals with no reduction of resistance under weak attacks and very minor reduction of resistance under strong adversarial attacks. Together with our model and algorithm selections and loss function design, we provide an integrated approach to produce robust DNNs with high efficiency and accuracy. Furthermore, we provide a missing benchmark on robustness of quantized models.

I. INTRODUCTION

A. Background

Deep Neural Networks (DNNs) have achieved significant success in computer vision and natural language processing. Especially, the residual network (ResNet)[11] has achieved remarkable performance on image classification and has become one of the most important neural network architectures in the current literature. Given an image dataset of N labeled images, $\mathcal{X} = \{(\mathbf{x}_1, y_1), \dots, (\mathbf{x}_n, y_n)\}$, a DNN f with parameters ω is trained to classify images by minimizing a object function \mathcal{L} formulated as

$$\mathcal{L}(\omega) = \frac{1}{N} \sum_{i=1}^N l(f(\omega, \mathbf{x}_i), y_i) \quad (1)$$

where l is a loss function that is typically chose to be the cross entropy loss. Despite the tremendous success of DNNs, researchers still try to strength two properties of DNNs, robustness and efficiency. In particular, for security-critic and on the edge applications. Robustness keeps the model accurate under small adversarial perturbation of input images, and efficiency enables us to fit DNNs into embedded system, such as smart-phone. Many adversarial defense algorithms [20], [10], [15],

[31] have been proposed to improve the robustness of DNNs. Among them, adversarial training is one of the most effective and powerful methods. Meanwhile, several adversarial attack scheme [9], [4], [1], [2] are proposed to break the existing adversarial defenses. Fast gradient sign method (FGSM) and iterative fast gradient sign method (IFGSM) [9] are amongst widely used to test the robustness of models by researchers. On the other hand, quantization [6], [22], producing models with low-precision weights, and structured simplification, such as channel pruning [12], [32], are promising ways to make models computationally efficient. Both methods above can significantly accelerate DNNs inference and reduce the memory requirement.

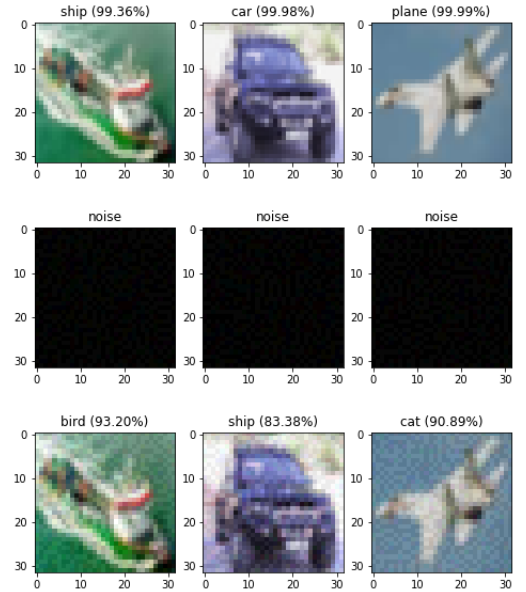


Fig. 1: First row: the original images labeled with the classification results by a ResNet56 and its confidence level. Second row: the perturbation (noise) generated by FGSM. Third row: the perturbed images labeled with classification results by the model as well as the model's confidence level. Minor noises that human eyes cannot even tell can affect DNNs significantly.

B. Our Contributions

Based on related works, we study the robustness of quantized models with binary weights under the adversarial training. We try to find the possibility to meet both robustness and efficiency, as well as the balance between natural accuracy and robust accuracy. Our work involves both experimental investigation and theoretical analysis.

Zhijian Li and Jack Xin are with Department of Mathematics, University of California, Irvine (e-mail: zhijl2@uci.edu; jack.xin@uci.edu).

Bao Wang is with Department of Mathematics and Scientific Computing and Imaging Insititute, The University of Utah (email: wang-baonj@gmail.com).

- Experimentally, we designed an integrated approach to produce robust model that is highly efficient for inference; in particular, aimed for on-device applications. This approach integrates model selection, algorithm selection, loss function selection, and sparsification.
- We make an improvement on a current state-of-the-art trade-off loss function initially proposed by [31], which increases both natural accuracy and robust accuracy. We also provide a theoretical interpretation that can explain why the improved trade-off loss function performs better.
- We discover that high precision quantization produces DNNs with sparse weights. We also investigate the structure of the sparsity and provide a method to produce quantized robust models with structured sparsity that can be further simplified by leveraging channel pruning.
- We benchmark the adversarial robustness of quantized models on several popular datasets, and we also provide the missing baseline results for possible future research.

C. Organization

We organize this work as following: In section 2, we introduced relevant concepts and important related works. In section 3, we investigate the robustness of binarized models on Cifar10, as well as the performances of BC versus BR. In section 4, we design a trade-off loss function to improve the natural accuracy of adversarially trained model on Cifar10 while minimizing the reduction on robustness. In section 5, we study the channel sparsity of high-precision quantized models. Based on our study, we improve the structureness of sprasity of quantized models. In section 6, we integrated all techniques studied above to produce robust quantized models and validate our work by generalizing this approach to MNIST, Fashion MNIST, SVHN, and Cifar100.

D. Notation

II. RELATED WORK

A. Binary Quantization

Based on the binary-connect (BC) [6] algorithm [30] proposed an improvement of BC called Binary-Relax, which makes the weights converge to the binary weights from the floating point weights gradually. Theoretically, [30] provided the convergence analysis of BC, and [16] presented an ergodic error bound of BC. The space of m-bit quantized weights $\mathcal{Q} \subset \mathbb{R}^n$ is a union of disjoint one-dimensional subspace of \mathbb{R}^n .

$$\mathcal{Q} = \mathbb{R}_+ \times \{\pm q_1, \dots, \pm q_m\}^n = \bigsqcup_{l=1}^p \mathcal{A}_l$$

We minimize our object function in the subspace \mathcal{Q} . Hence, the problem of binarizing weights can be formulated in the following two equivalent forms:

- I.

$$\operatorname{argmin}_{u \in \mathcal{Q}} \mathcal{L}(u)$$

- II.

$$\operatorname{argmin}_{u \in \mathbb{R}^n} \mathcal{L}(u) + \chi_{\mathcal{Q}}(u) \quad \text{where} \quad \chi_{\mathcal{Q}}(u) = \begin{cases} 0 & u \in \mathcal{Q} \\ \infty & \text{else} \end{cases} \quad (2)$$

Based on the above alternative form II, [30] relaxed the optimization problem to:

$$\operatorname{argmin}_{u \in \mathbb{R}^n} \mathcal{L}(u) + \frac{\lambda}{2} \operatorname{dist}(u, \mathcal{Q})^2 \quad (3)$$

Observing (3) converges to (2) pointwisely as $\lambda \rightarrow \infty$, therefore, [30] proposed a relaxation of BC:

$$\begin{cases} w_{t+1} = w_t - \gamma \nabla \mathcal{L}_t(u_t) \\ u_{k+1} = \operatorname{argmin}_{u \in \mathbb{R}^n} \frac{1}{2} \|w_{t+1} - u\|^2 + \frac{\lambda}{2} \operatorname{dist}(u, \mathcal{Q})^2 \end{cases}$$

where the second step is solved in closed form as following:

$$\begin{aligned} & \min_{u \in \mathbb{R}^n} \min_{z \in \mathcal{Q}} \frac{1}{2} \|w_{t+1} - u\|^2 + \frac{\lambda}{2} \|u - z\|^2 \\ & = \min_{z \in \mathcal{Q}} \min_{u \in \mathbb{R}^n} \frac{1}{2} \|w_{t+1} - u\|^2 + \frac{\lambda}{2} \|u - z\|^2 \end{aligned}$$

For fixed $z \in \mathcal{Q}$, the u that optimize the inner problem is $u = \frac{\lambda z + w_{t+1}}{\lambda + 1}$. Plug this optimal u into the problem, we solve the optimal $z = \operatorname{argmin}_{z \in \mathcal{Q}} \|z - w_{t+1}\|^2 = \operatorname{proj}(w_{t+1})$. Finally, the optimal u for this z is

$$u_{t+1} = \frac{\lambda \operatorname{proj}_{\mathcal{Q}}(w_{t+1}) + w_{t+1}}{\lambda + 1}$$

B. Adversarial Attacks

As [24] discovered the limited continuity of DNNs' input-output mapping, the outputs of DNNs can be changed by adding imperceptible adversarial perturbations to input data. The methods that generate perturbed data can be adversarial attacks, and the generated perturbed data are called adversarial examples. Here we introduce three benchmark adversarial attacks [9], [4]:

- 1) Fast gradient sign method (FGSM):

Given a specific magnitude of perturbation ϵ , FGSM searches adversarial examples by perturbing the input data towards gradient of loss function.

$$x' = x + \epsilon \cdot \nabla_w l(f(w, x), y)$$

- 2) Iterative FGSM (IFGSM):

Given an iteration number n , step size α , and a magnitude ϵ , IFGSM generates adversarial examples by perturbing the data towards the gradient of loss function iteratively and threshold the perturbation in each iteration, which leads to

$$x^{(n)} = x^{n-1} + \alpha \nabla_w \mathcal{L}(f(w, x^{(n-1)}), y)$$

for $n = 1, \dots, n$, and $x^{(0)} = x$. Then,

$$x' = x + \operatorname{Clip}_{\epsilon}(x^{(n)})$$

Algorithm 1 Binary-Relax quantization algorithm

```

1: Input: mini-batches  $\{(\mathbf{x}_1, \mathbf{y}_1), \dots, (\mathbf{x}_m, \mathbf{y}_m)\}$ ,  $\lambda_0 = 1$ , growth rate  $\rho > 1$ , learning rate  $\gamma$ , initial float weight  $w_0$ , initial
   binary weight  $u_0 = w_0$ , cut-off epoch  $M$ 
2: Output: a sequence of binary weights  $\{u_t\}$ 
3: for  $t = 1, \dots, N$  do ▷  $N$  is the number of epochs
4:   if  $t < M$  then
5:     for  $k = 1, \dots, m$  do
6:        $w_t = w_{t-1} - \gamma_t \nabla_k \mathcal{L}(u_{t-1})$ 
7:        $u_t = \frac{\lambda_t \cdot \text{Proj}_{\mathcal{Q}}(w_t) + w_t}{\lambda_t + 1}$ 
8:        $\lambda_{t+1} = \rho \cdot \lambda_t$ 
9:   else
10:    for  $k = 1, \dots, m$  do
11:       $w_t = w_{t-1} - \gamma_t \nabla \mathcal{L}(u_{t-1})$ 
12:       $u_t = \text{Proj}_{\mathcal{Q}}(w_t)$  ▷ This is precisely Binary-Connect
13: return quantized weights  $u_N$ 

```

where

$$\text{Clip}_{\epsilon}(x) = \begin{cases} \epsilon & x \geq \epsilon \\ x & -\epsilon < x < \epsilon \\ -\epsilon & x \leq -\epsilon \end{cases}$$

- 3) Carlini and Wagner method (C&W): C&W method provides adversarial examples by solving the problem

$$\min_{\delta} \|\delta\| \text{ s.t. } f(w, x + \delta) = t$$

for a target label t . While Carlini and Wagner originally proposed the metric $\|\cdot\|$ to be l_2 , most researchers use l_{∞} instead, which is a much stronger attack than C&W attack in the l_2 norm. In our study, we also use l_{∞} for C&W attack.

Among these 3 adversarial attacks with $\epsilon=0.031$, IFGSM is the strongest attack. IFGSM can make a ResNet56 with natural training predict all test data of Cifar10 wrong with confidence level at least 99.3% over all test images. C&W can reduce the test accuracy of ResNet56 on Cifar10 from 92% to 5.12%, and FGSM reduces the accuracy to 17.26%. While there are many more adversarial attack methods [14], [17], methods above are computationally efficient and are the most popular methods used to examine the robustness of models.

C. Adversarial Training

[8] rigorously established a rigorous benchmark to evaluate the robustness of machine learning models and investigated almost all current popular adversarial defense algorithms. They conclude that adversarially trained models outperform models with other types of defense methods in terms of resilient to adversarial attacks. [31] also shows that adversarial training is more powerful than other methods such as gradient mask and gradient regularization [15]. Adversarial training [1], [20] generates perturbed input data and train the model to stay stable under adversarial examples. It has the following object function:

$$\min_w \mathcal{L}(w) = \frac{1}{N} \sum_{n=1}^N \max_{\tilde{x}_n \in D_n} l(f(w, \tilde{x}_n), y_n) \quad (4)$$

where $D_n = \{x \mid \|x - x_n\|_{\infty} < \delta\}$. l and f are the loss function and the DNN respectively. In this work, we denote (1) to be \mathcal{R}_{nat} and (4) to be \mathcal{R}_{rob} . A widely used method to practically find \tilde{x}_n is the projected gradient decent (PGD) [20]. [23] investigated the properties of the object function of the adversarial training, and [28] provided convergence analysis of adversarial training based on the previous results.

Feynman-Kac formalism principled Robust DNNs: Neural ordinary differential equations (ODEs) [5] are a class of DNNs that use an ODE to describe the data flow of each input data. Instead of focusing on modeling the data flow of each individual input data, [27], [26], [18] use a transport equation (TE) to model the flow for the whole input distribution. In particular, from the TE viewpoint, [27] modeled training ResNet [11] as finding the optimal control of the following TE

$$\begin{cases} \frac{\partial u}{\partial t}(\mathbf{x}, t) + G(\mathbf{x}, \mathbf{w}(t)) \cdot \nabla u(\mathbf{x}, t) = 0, & \mathbf{x} \in \mathbb{R}^d, \\ u(\mathbf{x}, 1) = g(\mathbf{x}), & \mathbf{x} \in \mathbb{R}^d, \\ u(\mathbf{x}_i, 0) = y_i, & \mathbf{x}_i \in T, \text{ with } T \text{ being the training set.} \end{cases} \quad (5)$$

where $G(\mathbf{x}, \mathbf{w}(t))$ encodes the architecture and weights of the underlying ResNet, $u(\mathbf{x}, 0)$ serves as the classifier, $g(\mathbf{x})$ is the output activation of ResNet, and y_i is the label of \mathbf{x}_i .

[27] interpreted adversarial vulnerability of ResNet as arising from the irregularity of $u(\mathbf{x}, 0)$ of the above TE. To enhance $u(\mathbf{x}, 0)$'s regularity, they added a diffusion term, $\frac{1}{2}\sigma^2 \Delta u(\mathbf{x}, t)$, to the governing equation of (5) which resulting in the convection-diffusion equation (CDE). By the Feynman-Kac formula, $u(\mathbf{x}, 0)$ of the CDE can be approximated by the following two steps:

- Modify ResNet by injecting Gaussian noise to each residual mapping.
- Average the output of n jointly trained modified ResNets, and denote it as $\text{En}_n \text{ResNet}$.

[27] have noticed that EnResNet can improve both natural and robust accuracies of the adversarially trained DNNs. In this work, we leverage the sparsity advantage of EnResNet to push the sparsity limit of the adversarially trained DNNs.

TRADES: It is well-known that adversarial training will significantly reduce the accuracy of models on clean images.

For example, ResNet20 can achieve about 92% accuracy on CIFAR10 dataset. However, under the PGD training using $\epsilon = 0.031$ with step-size 0.007 and the number of iterations 10, ResNet20 only has 76% accuracy on clean images of CIFAR10. [31] designed a trade-off loss function, TRADES, that balances the natural accuracy and adversarial accuracy. The main idea of TRADES is to minimize the difference of adversarial error and the natural error:

$$\mathcal{R}_{rob}(f) - \mathcal{R}_{nat}^*$$

where $\mathcal{R}_{nat}^* = \min_f \mathbb{E}[\phi(f(X)Y)]$ with a loss function ϕ . [31] theoretically showed that

$$\mathcal{R}_{rob} - \mathcal{R}_{nat}^* < \psi^{-1}(\mathcal{R}_{\phi} - \mathcal{R}_{nat}^*) + \mathbb{E} \max_{X' \in \mathbb{B}(X, \epsilon)} \phi(f(X)f(X')\lambda) \quad (6)$$

ψ is a functional transformation introduced by [3]. Based on (6), they proposed the following TRADES loss function

$$\min_f \mathbb{E} \left(\phi(f(X)Y) + \max_{X' \in \mathbb{B}(X, \epsilon)} \phi(f(X)f(X')\lambda) \right) \quad (7)$$

TRADES is considered to be the state-of-the-art adversarial defense method, it outperforms most defense methods in both robust accuracy and natural accuracy. [8] investigated various defense methods, and TRADES performs the best among them. TRADES will provide important baselines in this work.

III. QUANTIZATION OF ENRESNET

We know that the accuracy of a quantized model will be lower than its counterpart with floating point weights because of loss of precision. However, we want to know that whether a quantized model is more vulnerable than its float equivalent under adversarial attacks? In this section, we study this question by comparing the accuracy drops of the natural accuracy and robust accuracy from float weights to binary weights. Meanwhile, we also investigate the performances between two quantization methods BC and BR.

A. Experimental Setup

Dataset. We use one of the most popular datasets CIFAR-10 [13] to evaluate the quantized models, as it would be convenient to compare it with the float models used in [27], [31].

Baseline. For model, our baseline model is the regular ResNet. Since, as the best of our knowledge, there are no suitable work done before that investigated the robustness of models with quantized weights. We mainly look at that how close our quantized models can be to the float models [27], [31].

Evaluation. We evaluate both natural and robust accuracies for quantized adversarial trained models. We examine the robustness of models by three attack methods, FGSM (A_1), IFGSM (A_2), and C&W (A_3). In our recording, N denotes the natural accuracy (accuracy on clean images) of models. For FGSM, we use $\epsilon = 0.031$ as almost all works share this value for FGSM. For IFGSM, we use $\alpha = 1/255$, $\epsilon = 0.031$, and number of iterations 20. For C&W, we have learning rate 0.0006 and number of iterations 50.

Algorithm and Projection For algorithm, we set the BC as our baseline, and we want to find that whether the advantage of the relaxed algorithm 1 in [30] is preserved under adversarial training. In both BC and BR, we use the widely used binarizing projection proposed by [22], namely:

$$\text{Proj}_{\mathcal{Q}}(w) = \mathbb{E}[|w|] \cdot \text{sign}(w) = \frac{\|w\|_1}{n} \cdot \text{sign}(w)$$

where $\text{sign}(\cdot)$ is the component-wise sign function and n is the dimension of weights.

B. Result

First, we see that the quantized models can maintain decent robustness under the attacks. The drops of the robust accuracies are roughly in the same amount as the natural accuracy (Table I), which indicates that quantization does not make the model more vulnerable.

Second, we investigate the performances of Binary-Connect method (BC) and Binary-Relax method (BR). We verify that BR outperforms BC (Table I). A quantized model trained via BR provides higher natural accuracy and robust accuracy. As a consequence, we use this relaxed method to quantize DNNs in all subsequent experiments in this paper.

Finally, We verify that the EnResNet is more robust com-

Model	Quant	N	A_1	A_2	A_3
En1 ResNet20	Float	78.31%	56.64%	49.00%	66.84%
	BC	68.84%	46.31%	42.45%	58.52%
	BR	69.60%	47.17%	43.89%	58.79%
En2 ResNet20	Float	80.10%	57.48%	49.55%	66.73%
	BC	71.48%	47.83%	43.03%	59.09%
	BR	72.58%	49.29%	44.72%	60.36%
En5 ResNet20	Float	80.64%	58.14%	50.32%	66.96%
	BC	75.54%	51.03%	46.01%	60.92%
	BR	75.40%	51.60%	46.91%	61.52%

TABLE I: Binary Connect vs Binary Relax. Models quantized by Binary-Relax have higher natural accuracy and adversarial accuracies than those quantized by Binary-Connect

paring to the ResNet with the samiliar number of parameters under quantization. We train two sets of EnResNet and ResNet with adversarial training. As shown in table II, EnResNet has much higher robust accuracy for both float and quantized models. We also study the behavior of quantized models under black-box attacks. Suppose we have a target model and an oracle model. We test a quantized target network by three different blind attacks. The oracle models are the float equivalent of the target model, a quantized model with different architecture (to the target model), and a float model with different architecture respectively. The results are shown in Table III. As expected, the accuracies of models are improved significantly compared to those under white-box attacks. Moreover, we find out that if a black-box attack generates adversarial examples based on another binarized model, it will be more effective on attacking the target binarized model.

C. Adaptation of the existing analysis of BC to adversarial training

Researchers have established quite a few theoretical results on the stability of training binarized DNNs and error bounds

net(#params)	model	N	A_1	A_2	A_3
En ₁ ResNet20 (0.27M)	Float	78.31%	56.61%	49.00%	66.84%
	BR	69.60%	47.17%	43.89%	58.79%
ResNet20 (0.27M)	Float	76.30%	51.19%	46.72%	57.90%
	br	66.81%	43.37%	40.72%	52.14%
En ₂ ResNet20 (0.54M)	Float	80.10%	57.48%	49.36%	66.73%
	BR	72.58%	49.29%	44.72%	60.36%
ResNet34 (0.56M)	Float	77.82%	54.05%	49.89%	61.38%
	BR	70.31%	46.42%	43.26%	54.75%

TABLE II: Ensemble ResNet vs ResNets. We verify that EnResNet outperforms ResNet with the similar number of parameters with both float and binary weights.

Target	Oracle	A_1	A_2	A_3
En ₂ ResNet20	En ₂ ResNet20 Float	62.88%	55.65%	66.06%
En ₂ ResNet20	En ₃ ResNet20 Binary	55.18%	52.74%	64.82%
En ₂ ResNet20	En ₁ ResNet56 Float	63.58%	56.59%	66.83%
En ₁ ResNet56	En ₁ ResNet56 Float	62.30%	58.05%	68.14%
En ₁ ResNet56	En ₁ ResNet20 Binary	59.96%	55.54%	66.14%
En ₁ ResNet56	En ₁ ResNet20 Float	63.58%	58.72%	69.82%

TABLE III: Robustness of binarized models under Black Box Attack. Models achieve much higher accuracies than being attacked by white-box attacks in Table I. Black-box attacks target on another binary model are more effective than those on float models

of DNNs with binary weights. We note that these theoretical analysis of quantization under natural training can be adapted to the adversarial training.

We use $h(w, x_n)$ to denote $\max_{\tilde{x}_n \in D_n} l(f(w, \tilde{x}_n), y_n)$. Hence, we can rewrite (4) more concisely as:

$$\min_w \mathcal{L}(w) = \frac{1}{N} \sum_{n=1}^N h(w, \mathbf{x}_n)$$

In the subsequent analysis, we first introduce a few common assumptions used in analysis of DNNs.

Assumptions:

- 1) h is Lipschitz differentiable in both arguments. i.e. $\exists C > 0$, s.t.
 $\sup_{\mathbf{x}} \|\nabla_w h(w_1, \mathbf{x}) - \nabla_w h(w_2, \mathbf{x})\| \leq C \|w_1 - w_2\|$
 $\sup_w \|\nabla_w h(w, \mathbf{x}_1) - \nabla_w h(w, \mathbf{x}_2)\| \leq C \|\mathbf{x}_1 - \mathbf{x}_2\|$
 $\sup_{\mathbf{x}} \|\nabla_{\mathbf{x}} h(w_1, \mathbf{x}) - \nabla_{\mathbf{x}} h(w_2, \mathbf{x})\| \leq C \|w_1 - w_2\|$
- 2) The variance of the stochastic gradients is bounded. i.e. $\mathbb{E}[\|\nabla \mathcal{L}(w) - \nabla \mathcal{L}_k(w)\|^2] \leq \sigma^2, \forall k \in \mathbb{N}$, where $\nabla \mathcal{L}_k(w)$ is the sampled mini-batch gradient at k -th epoch.
- 3) $h(w, \mathbf{x})$ is locally strongly concave in \mathbf{x} in all D_n . That is, $\exists \mu > 0$ s.t. $\forall n$ and $\mathbf{x}_1, \mathbf{x}_2 \in D_n$, we have
 $h(w, \mathbf{x}_1) \geq h(w, \mathbf{x}_2) + \langle \nabla_{\mathbf{x}} h(w, \mathbf{x}_2), \mathbf{x}_1 - \mathbf{x}_2 \rangle - \frac{\mu}{2} \|\mathbf{x}_1 - \mathbf{x}_2\|^2$

Lipschitz differentiable and bounded variance assumptions of the stochastic gradients are common assumptions [30], [16], [28], [23] made for analysis of the gradient descent. Assumption 3, made according to [23], [28], is the additional assumption to adapt the situation to robust training.

Lemma 1 (lemma 1 in [28]). *Under Assumptions 1) and 3), we have \mathcal{L} is L -Lipschitz differentiable*

$$\|\nabla \mathcal{L}(w_1) - \nabla \mathcal{L}(w_2)\| \leq L \|w_1 - w_2\|$$

then consequently,

$$\mathcal{L}(w_1) \leq \mathcal{L}(w_2) + \langle \nabla \mathcal{L}(w_2), w_1 - w_2 \rangle + \frac{L}{2} \|w_1 - w_2\|^2$$

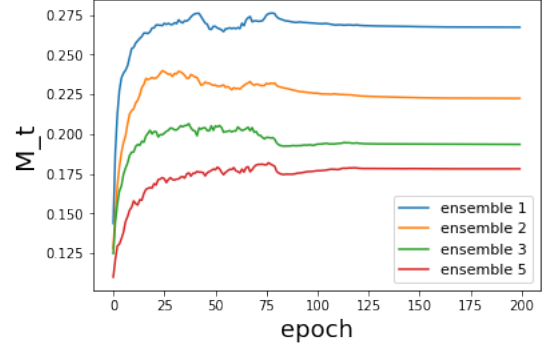


Fig. 2: Maximum of Binary Weights under l_1 norm against epochs

$$\text{where } L = \frac{C^2}{\mu} + C$$

Lemma 1 shows that if the original loss function is Lipschitz differentiable, with a few additional conditions, the loss function of the adversarial training is also Lipschitz differentiable. This result allows us to extend many existing analysis of quantization to adversarial training. In particular, the following theorem provided in [16] holds for the adversarial training.

Theorem 1 (Theorem 3 in [16]). *Let $w^* = \operatorname{argmin}_{w \in R^n} \mathcal{L}(w)$ and learning rate $\gamma_t = 1/t$. Assume that the domain of \mathcal{L} is bounded with diameter D . \mathcal{L} is convex and satisfies the assumptions 1,2 and 3, then the ergodic error satisfies*

$$\lim_{T \rightarrow \infty} \mathbb{E}[\mathcal{L}(\bar{w}_T) - \mathcal{L}(w^*)] \leq 2\sqrt{n}MLD$$

where $\bar{w}_T = \frac{1}{T} \sum_{t=1}^T w_t$, L and M are the constants in Lemma 1 and $\limsup_t \mathbb{E}[\|w_t\|]$ respectively, and n is the dimension of the domain.

Network	M
En ₁ ResNet20	0.2762
En ₂ ResNet20	0.2399
En ₃ ResNet20	0.2065
En ₅ ResNet20	0.1819

TABLE IV: The uniform bound M . The ruining maximum of M_t recorded in training decreases as the number of ensemble increases.

One drawback of this theorem is that whether M is bounded or not remains unknown to us. Therefore, we numerically investigate the values of M , and we uncover an interesting feature of ensemble ResNet. Let \mathcal{W}_t be collection of convolutional layers of the neural network at epoch t . Define

$$M_t = \max_{w \in \mathcal{W}_t} E(|w|), \quad M = \max_{\substack{1 \leq t \leq T \\ w \in \mathcal{W}_t}} \mathbb{E}(|w|) = \max_{1 \leq t \leq T} M_t$$

Namely, M_t is the layer with the maximum of absolute mean at epoch t , and M is the running maximum of M_t over all epochs. Since we train each model 200 epochs, we have $T = 200$ here. We find that M is numerically bounded (as in Fig. 2) and small. Moreover, the value of M decreases as the number of ensembles increases (Table IV). In other words, the bound provided by theorem 1 is tighter when the

number of ensembles is larger. From Table 3, we see that, for both quantized and float model the kernels have the smaller weights for the larger number of ensembles. A pervious work that studied the sparsity of EnResNet [7] also found a similar result that the weights of EnResNet are smaller for a larger number of ensembles. Theorem 1 offers an explanation that how this feature of EnResNet can favor its performance. In addition, [30] provided the analysis of stability of algorithm 1, and [19] presented the convergence of quantization. Thanks to Lemma 1, we can extend those results to adversarial training.

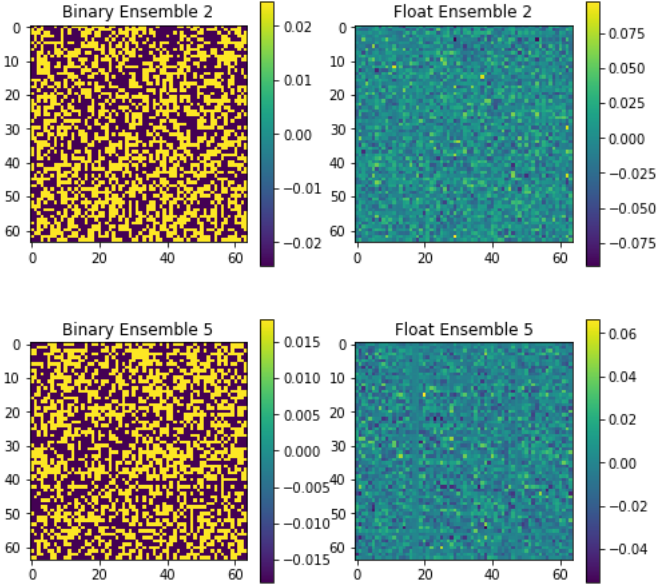


Fig. 3: Visualizations of float and quantized kernels: left-hand side columns are randomly selected kernels of quantized models, and the right-hand columns are the same kernels of float models. We turn the float weights into binary using Algorithm 1.

IV. TRADE-OFF BETWEEN ROBUST ACCURACY AND NATURAL ACCURACY

A. Previous work and our methodology

It is known that adversarial training will decrease the accuracy for classifying the clean input data. This phenomenon is verified both theoretically [25] and experimentally [31], [27], [15] by researchers. [31] proposed a trade off loss function (7) for robust training to balance the adversarial accuracy and natural accuracy. In practice, it formulated as following:

$$\mathcal{L} = \mathcal{L}_{nat} + \beta \cdot \frac{1}{N} \sum_{n=1}^N l(f(x_n), f(\tilde{x}_n)) \quad (8)$$

The Motivated by [31], we study the following trade-off loss function for our quantized models:

$$\mathcal{L} = \alpha \cdot \mathcal{L}_{nat} + \beta \cdot \mathcal{L}_{rob} \quad (9)$$

Note that adversarial training is a special case $\alpha = 0$, $\beta = 1$ in (9). TRADES, the loss function (8), improves the robustness of models by pushing the decision boundary

away from the original data points, clean images in this case. However, intuitively, if the model classifies a original data point wrong, the second term of (8) will still try to extend this decision boundary, which can prevent the first term of the loss function from leading the model to the correct classification. In this section, we will experimentally compare (8) and (9) and theoretically analyze the difference between them.

B. Experiment and result

To compare the performances of two loss functions, we choose our neural network and dataset to be En₁ResNet20 and CIFAR-10, respectively. Based on [31], who studied β of (8) in the range $[1, 10]$, we vary the trade-off parameter β , the weight of adversarial loss, in the set $[1, 4, 8]$ to emphasize the robustness in different levels.

The experiment results are listed in Table V. We observe that, when the natural loss and the adversarial loss are equally treated, (8) focuses on the natural accuracy while (9) favors on the robust accuracy. As the trade-off parameter β increases, (8) trades quite amount of natural loss for robustness, while (9) trades a relatively small amount of natural loss for robustness. Furthermore, we find that (9) has better trade-off efficiency. Hence, we say that the loss function (9) outperforms (8).

C. Analysis of trade-off functions

Let us consider the binary classification case, where have our samples $(\mathbf{x}, y) \in \mathcal{X} \times \{-1, 1\}$. Let $f : \mathcal{X} \rightarrow \mathbb{R}$ be a classifier and $\sigma(\cdot)$ be an activation function. Then our prediction for a sample is $\hat{y} = \text{sign}(f(\mathbf{x}))$ and the corresponding score is $\sigma(f(\mathbf{x}))$. Above is the theoretical setting provided by [31]. Then, we have the errors $\mathcal{R}_\phi(f)$ and $\mathcal{R}_\phi^*(f)$ corresponding to (8) and (9) respectively, considering $\alpha = \beta = 1$ for both loss functions:

$$\begin{aligned} \mathcal{R}_\phi(f) &= \mathbb{E}[\phi(\sigma \circ f(\mathbf{x}) \cdot y)] + \mathbb{E}[\phi(\sigma \circ f(\mathbf{x}) \cdot \sigma \circ f(\mathbf{x}'))] \\ \mathcal{R}_\phi^*(f) &= \mathbb{E}[\phi(\sigma \circ f(\mathbf{x}) \cdot y)] + \mathbb{E}[\phi(\sigma \circ f(\mathbf{x}') \cdot y)] \end{aligned}$$

We first consider the simple case that ϕ is the 0-1 loss function. Then, we don't need a activation function in this case so we take $\sigma(\theta) = \theta$.

Proposition 1. Let ϕ be the 0-1 loss function and activation function be the identity map. Then,

$$\mathcal{R}_\phi(f) \leq \mathcal{R}_\phi^*(f)$$

Proof: We first define a set E :

$$E = \{\mathbf{x} | f(\mathbf{x})y < 0, f(\mathbf{x}')y > 0\}$$

By the definition of adversarial examples in (4),

$$\mathbb{E}[\mathbf{1}\{E\}] = 0$$

where $\mathbf{1}\{E\}$ is the indicator function of the set. That is, the set that the classifier predicts original data point wrong but the perturbed data point correctly should have measure 0. Now, we define the following sets:

$$B = \{\mathbf{x} | f(\mathbf{x})y \geq 0, f(\mathbf{x}')y \geq 0\}$$

Model	Loss	N	A_1	A_2	A_3
En ₁ ResNet20	(8) ($\beta = 1$)	84.49%	45.96%	34.81%	51.94%
En ₁ ResNet20	(9) ($\alpha = 1, \beta = 1$)	83.47%	54.46%	43.86%	64.04%
En ₁ ResNet20	(8) ($\beta = 4$)	80.05%	51.24%	45.43%	58.85%
En ₁ ResNet20	(9) ($\alpha = 1, \beta = 4$)	80.91%	55.92%	47.17%	66.53%
En ₁ ResNet20	(8) ($\beta = 8$)	75.82%	51.63%	46.95%	59.31%
En ₁ ResNet20	(9) ($\alpha = 1, \beta = 8$)	79.31%	56.28%	48.02%	66.07%

TABLE V: Comparison of Loss Function. Trade-off loss function (8) outperforms TRADES (9) in most cases.

Model	loss	N	A_1	A_2	A_3
En ₁ ResNet20	$\alpha = 0, \beta = 1$	69.60%	47.81%	43.89%	58.79%
En ₁ ResNet20	$\alpha = 1, \beta = 4$	73.40%	47.41%	41.86%	57.83%
En ₁ ResNet20	$\alpha = 1, \beta = 8$	71.35%	47.42%	42.46%	59.01%
En ₂ ResNet20	$\alpha = 0, \beta = 1$	71.58%	49.29%	44.62%	60.36%
En ₂ ResNet20	$\alpha = 1, \beta = 4$	75.92%	48.97%	43.41%	59.40%
En ₂ ResNet20	$\alpha = 1, \beta = 8$	74.72%	49.66%	43.96%	60.65%
En ₅ ResNet20	$\alpha = 0, \beta = 1$	75.40%	51.60%	46.91%	61.52%
En ₅ ResNet20	$\alpha = 1, \beta = 4$	78.50%	50.85%	45.02%	60.96%
En ₅ ResNet20	$\alpha = 1, \beta = 8$	77.35%	51.62%	45.63%	61.11%

TABLE VI: Trade-off loss function for binarized models with different parameters. When $\alpha = 1$ and $\beta = 8$, models can achieve about the same accuracies under FGSM and C&W attacks as adversarially trained models, while the natural accuracy is improved.

$$D = \{\mathbf{x} | f(\mathbf{x})y \geq 0, f(\mathbf{x}')y < 0\}$$

$$F = \{\mathbf{x} | f(\mathbf{x})y < 0, f(\mathbf{x}')y < 0\}$$

We note that

$$\{\exists \mathbf{x}' \in \mathbf{B}(\mathbf{x}, \delta) \ f(\mathbf{x}')f(\mathbf{x}) \leq 0\} = D \cup E$$

$$\{\exists \mathbf{x}' \in \mathbf{B}(\mathbf{x}, \delta) \ f(\mathbf{x}')y \leq 0\} = D \cup F$$

Then

$$\mathbb{E}[\mathbf{1}\{\exists \mathbf{x}' \in \mathbf{B}(\mathbf{x}, \delta) \ f(\mathbf{x}')f(\mathbf{x}) \leq 0\}] = \mathbb{E}[\mathbf{1}\{D\}]$$

$$\leq \mathbb{E}[\mathbf{1}\{D\} + \mathbf{1}\{F\}] = \mathbb{E}[\mathbf{1}\{\exists \mathbf{x}' \in \mathbf{B}(\mathbf{x}, \delta) \ f(\mathbf{x}')y \leq 0\}]$$

As we consider the naive 0-1 loss, both loss functions have no penalty on set B . Therefore, we have

$$\begin{aligned} \mathcal{R}_\phi(f) &= \mathbb{E}[\mathbf{1}\{f(\mathbf{x})y \leq 0\} + \mathbf{1}\{\exists \mathbf{x}' \in \mathbf{B}(\mathbf{x}, \delta) \ f(\mathbf{x}')f(\mathbf{x}) \leq 0\}] \\ &\leq \mathbb{E}[\mathbf{1}\{f(\mathbf{x})y \leq 0\} + \mathbf{1}\{\exists \mathbf{x}' \in \mathbf{B}(\mathbf{x}, \delta) \ f(\mathbf{x}')y \leq 0\}] = \mathcal{R}_\phi^*(f) \end{aligned}$$

□

The take away from these results is that under the same classifier, loss function and activation function, $\mathcal{R}_\phi^*(f)$ captures more errors than $\mathcal{R}_\phi(f)$, as the later fails to capture the robust error when the natural prediction is incorrect.

The same result also holds in more general cases. Now, we consider several common loss functions: the hinge loss ($\phi(\theta) = \max\{1 - \theta, 0\}$), the sigmoid loss ($\phi(\theta) = 1 - \tanh \theta$), and the logistic loss ($\phi(\theta) = \log_2(1 + e^{-\theta})$). Note that we want a loss function to be monotonic decreasing in $[-1, 1]$ as -1 indicates completely wrong and 1 indicates completely correct. Since our classes is 1 and -1 , we will choose hyperbolic tangent as our activation function.

Proposition 2. Let ϕ be any loss function that is monotonic decreasing on $[-1, 1]$ (all loss functions mentioned above

satisfy this), and $\sigma(\theta) = \tanh \theta$. Define $B = \{\mathbf{x} | f(\mathbf{x})y \geq 0, f(\mathbf{x}')y \geq 0\}$ as in proposition 1. Then:

$$\mathcal{R}_\phi(f) \geq \mathcal{R}_\phi^*(f) \text{ on } B \text{ and } \mathcal{R}_\phi(f) \leq \mathcal{R}_\phi^*(f) \text{ on } B^C$$

Proof: Let E , D , and F be the sets defined in proposition 1. We note that the activation function $\sigma(x)$ preserves the sign of x , and $|\sigma(x)| \leq 1$.

On the set B , $f(\mathbf{x})$, $f(\mathbf{x}')$, and y have the same sign, so are $\sigma(f(\mathbf{x}))$, $\sigma(f(\mathbf{x}'))$ and y . Therefore

$$\phi(\sigma(f(\mathbf{x}')) \cdot \sigma(f(\mathbf{x}))) \geq \phi(\sigma(f(\mathbf{x}') \cdot y))$$

as $0 \leq \sigma(f(\mathbf{x}')) \cdot \sigma(f(\mathbf{x})) \leq \sigma(f(\mathbf{x}')) \cdot y$. This shows

$$\mathcal{R}_\phi(f) \geq \mathcal{R}_\phi^*(f) \text{ on } B$$

We note that $B^C = E \cup D \cup F$. Since set E has measure zero, we only consider D and F .

On D , as f classifies \mathbf{x} correct and \mathbf{x}' wrong, we have

$$\sigma(f(\mathbf{x}')) \cdot y \leq \sigma(f(\mathbf{x}')) \cdot \sigma(f(\mathbf{x})) \leq 0$$

$$\Rightarrow \phi(\sigma(f(\mathbf{x}')) \cdot \sigma(f(\mathbf{x}))) \leq \phi(\sigma(f(\mathbf{x}') \cdot y))$$

On F , as f classifies both \mathbf{x} and \mathbf{x}' wrong, we have

$$\sigma(f(\mathbf{x}')) \cdot y \leq 0 \leq \sigma(f(\mathbf{x}')) \cdot \sigma(f(\mathbf{x}))$$

$$\Rightarrow \phi(\sigma(f(\mathbf{x}')) \cdot \sigma(f(\mathbf{x}))) \leq \phi(\sigma(f(\mathbf{x}') \cdot y))$$

In summary, we have

$$\mathcal{R}_\phi(f) \leq \mathcal{R}_\phi^*(f) \text{ on } B^C$$

□

In the more general case of proposition 2, we partition our space into several sets based on a given classifier f , and we examine the actions of loss functions on those sets. We see that (8) penalize set B heavier than (9), but the classifier classifies both the natural data and the perturbed data correct on B . On the other hand, (8) does not penalize sets E and F , where the classifier makes mistakes, enough, especially on set F . Therefore, (9) as a loss function is more on target. Based on both experimental results and theoretical analysis, we believe (9) is a better choice to balance natural accuracy and robust accuracy.

As our experiments on the balance of accuracies with different parameters in our loss function (9) in table VI. We find that it is possible to increase the natural accuracy while maintaining the robustness under relatively weak attacks (FGSM & CW), as the case of $\alpha = 1$ and $\beta = 8$ in table VI. However, the resistance under relatively strong attack (IFGSM) will inevitably decrease when we trade-off.

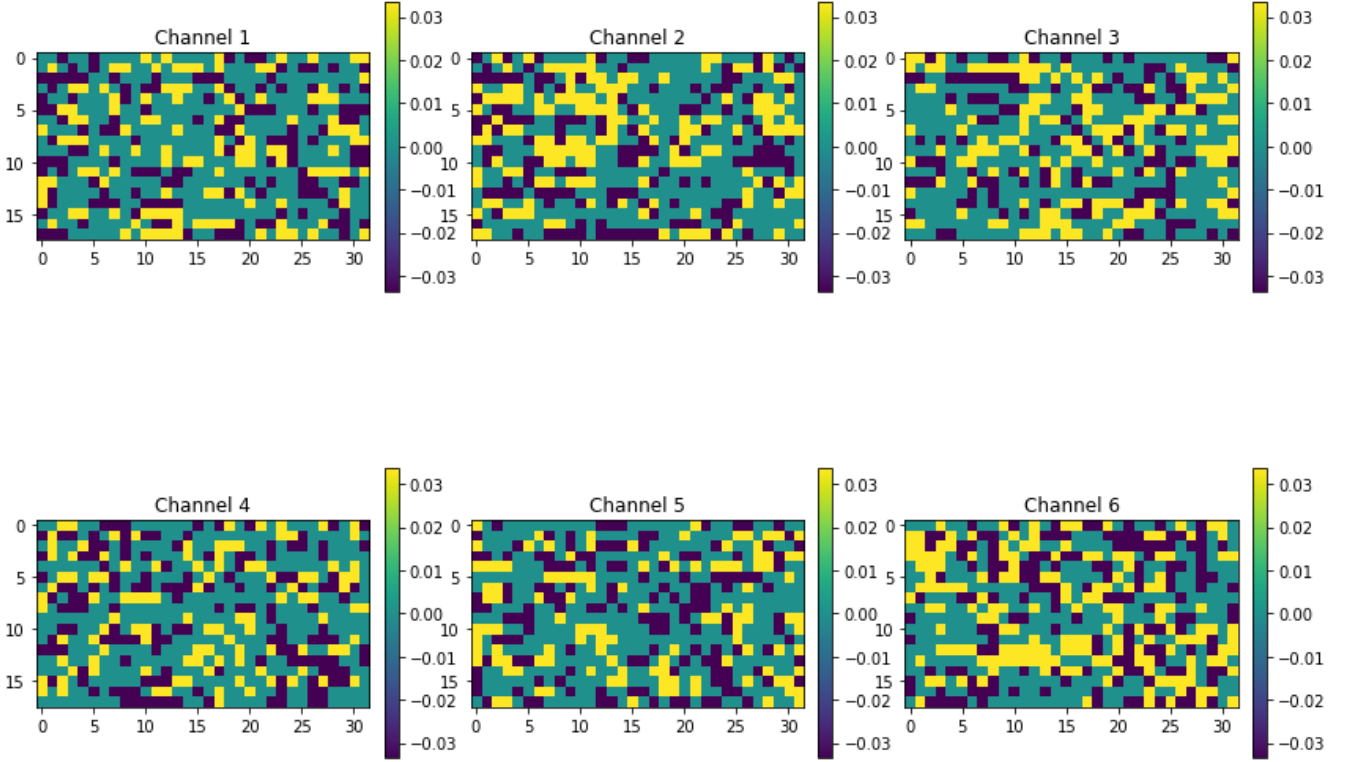


Fig. 4: Visualization of 4 ternary channels (reshaped for visualization) of a layer in ResNet20 under AT. The green areas are 0 weights.

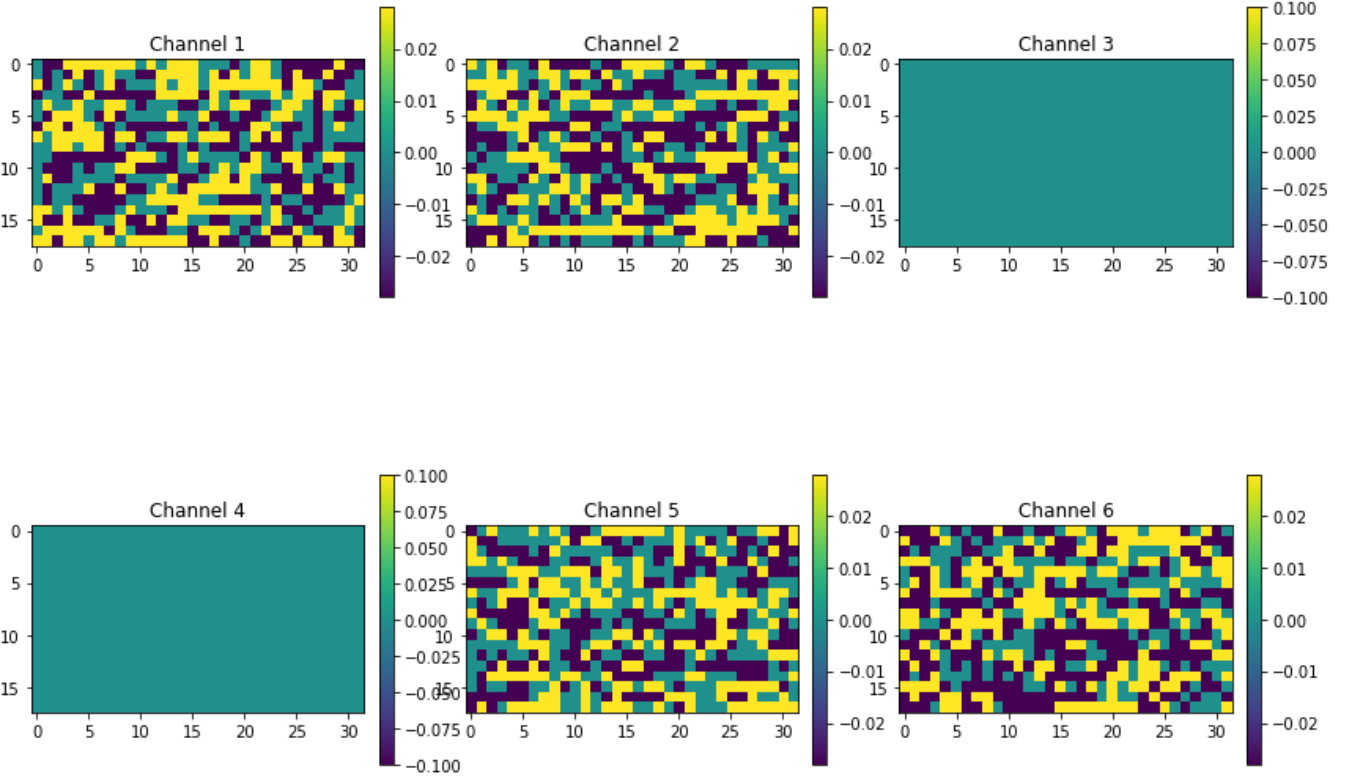


Fig. 5: Visualization of 4 ternary channels (reshaped for visualization) of a layer in $\text{En}_1\text{ResNet56}$ under natural training. There are less 0 weights in non-sparse channels. Nonzero weights of ternary channels under natural training are more concentrated. As a result, there are more sparse channels under natural training.

Model	Quant	Loss	Weight Sparsity	Channel Sparsity	N	A_1	A_2
ResNet20	tnn	Natural	53.00%	11.16%	90.54%	12.71%	0.00%
En ₁ ResNet20	tnn	Natural	52.19%	9.57%	90.61%	26.21%	0.71%
ResNet20	tnn	AT	50.71%	2.55%	68.30%	44.80%	42.53%
En ₁ ResNet20	tnn	AT	50.31%	4.14%	71.30%	48.17%	43.27%
En ₁ ResNet20	tnn	(9)	55.66%	7.02%	73.05%	48.10%	42.65%
ResNet20	4-bit	Natural	42.79%	9.53%	91.75%	12.38%	0.00%
En ₁ ResNet20	4-bit	Natural	44.73%	10.52%	91.42%	27.99%	0.62%
ResNet20	4-bit	AT	43.93%	2.55%	71.49%	47.63%	44.08%
En ₁ ResNet20	4-bit	AT	48.35%	4.94%	73.05%	51.43%	45.10%
En ₁ ResNet20	4-bit	(9)	55.57%	7.42%	76.61%	51.92%	44.39%
ResNet56	tnn	Natural	60.96%	31.86%	91.91%	15.58%	0.00%
En ₁ ResNet56	tnn	Natural	60.66%	28.97%	91.46%	38.22%	0.36%
ResNet56	tnn	AT	54.21%	15.37%	74.56%	51.73%	46.62%
En ₁ ResNet56	tnn	AT	54.70%	16.74%	76.87%	53.16%	47.89%
En ₁ ResNet56	tnn	(9)	58.89%	21.36%	77.24%	52.96%	46.01%
ResNet56	4-bit	Natural	67.94%	39.16%	93.09%	16.02%	0.00%
En ₁ ResNet56	4-bit	Natural	71.07%	41.10%	92.39%	39.79%	0.33%
ResNet56	4-bit	AT	55.29%	17.10%	77.67%	52.43%	48.22%
En ₁ ResNet56	4-bit	AT	55.09%	18.11%	78.25%	55.48%	49.03%
En ₁ ResNet56	4-bit	(9)	67.31%	33.18%	79.44%	55.41%	47.80%

TABLE VII: Sparsity and structure of sparsity of quantized models. We use $\alpha = 1$ and $\beta = 8$ in trade-off loss (9). While models under both natural training and adversarial have large proportion of sparse weights, sparsity of adversarially trained models are much less structured. Trade-off loss function (7) can improve the structure.

V. FURTHER BALANCE OF EFFICIENCY AND ROBUSTNESS: STRUCTURED SPARSE QUANTIZED NEURAL NETWORK VIA TERNARY/4-BIT QUANTIZATION AND TRADE-OFF LOSS FUNCTION

A. Sparse neural network delivered by high precision quantization

If we quantize DNNs with higher precision than binary quantization, such as ternary and 4-bit quantization. Then, the quantized weights are allowed to be 0. In fact, we find that a large proportion of weights will be 0 for quantized models. This suggests that a ternary or 4-bit quantized model can be further simplified via channel pruning. However, such simplification requires structure sparsity of DNN architecture. In our study, we use the algorithm 1 as before with the projection replaced by ternary and 4-bit respectively. As shown in Table VII, we find that sparsity of quantized DNNs under regular training are significantly more structured than those under adversarial training. For both ternary(tnn) and 4-bit quantization, quantized models with adversarial training have very unstructured sparsity, while models with natural training have much more structured sparsity. We verify this phenomenon for both ResNet20, En₁ResNet20, ResNet56, and En₁ResNet56 on Cifar10 Dataset. For example, 50.71% (0.135M out of 0.268M) of weights in convolutional layers are 0 in a ternary quantized ResNet20, but there are only 2.55% (16 out of 627) channels are 0. If the sparsity is unstructured, it is less useful for model simplification as channel pruning cannot be applied. A fix to this problem is our trade-off loss function, as factor natural loss into adversarial training should improve the structure of sparsity. Our experiment (Table VII) shows that a small factor of natural loss, $\alpha = 1$ and β in (9), can push the sparsity to be more structured. Meanwhile, the deepness of models also has an impact on the structure of sparsity. The deeper the more structured the sparsity is. We see in Table VII that, under the same settings, the structure of sparsity increases as the model becomes deeper. Figure

4 and figure 5, shows the difference between a unstructured sparsity of a ternary ResNet20 with adversarial training and a much more structured sparsity of ResNet56 with natural training. The trade-off function not only improves the natural accuracy of models with minor harm to robustness but also structure the sparsity of high precision quantization, so further simplification of models can be done through channel pruning.

VI. BENCHMARKING ADVERSARIAL ROBUSTNESS OF QUANTIZED MODEL

Based on previous discussions, integrating the relaxation algorithm, ensemble ResNet, and our trade-off loss function, we can produce very efficient DNN models with high robustness. To our best knowledge, there is no previous work that systematically study the robustness of quantized models. As a result, we do not have any direct baseline to measure our results. Therefore, we benchmark our results by comparing to models with similar size and current state-of-the-art defense methods. We verify that the performance of the quantized model with our approach on popular datasets, including Cifar 10, Cifar 100 [13], MNIST, Fashion MNIST (FMNIST) [29], and SVHN [21]. Among these datasets, MNIST and Fashion-MNIST are digital images with only one channel, i.e. black-and-white, and, therefore, are much easier to learn than CIFAR10. The Street View House Numbers(SVHN) datasets are images with three RGB channels, color digital images, like CIFAR10. In our experiments, we learn SVHN dataset without utilizing its extra training data. Our results are displayed in Table VIII. In this table, size refers to the number of parameters. We find that quantization has very little impact on learning small datasets MNIST and FMNIST. En₂ResNet20 and ResNet40 have about the same performance while the previous is binarized. In fact, En₂ResNet20 have about the same performance as its float equivalent, which means we get efficiency for 'free' on these small datasets. We benchmark the robustness of quantized models on large datasets, SVHN,

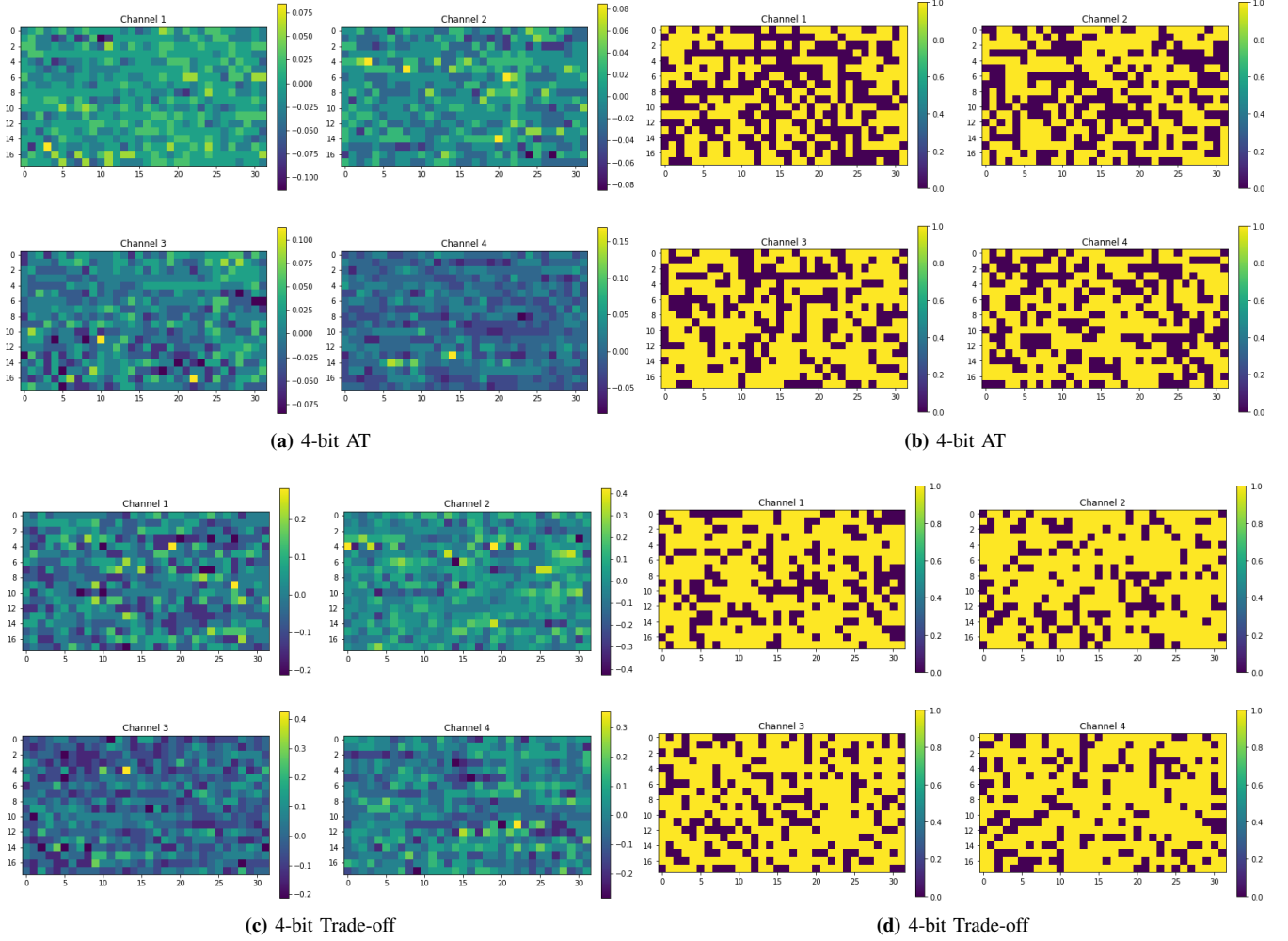


Fig. 6: Comparison of Adversarial training (AT) with trade-off loss: the left-hand side are original plots of channels, and we isolate the zero weights and nonzero weights of the left-hand side channels for better visualization in right-hand side. The dark parts are zero weights and the yellow parts are nonzero weights. We observe that the trade-off loss concentrates nonzero weights into non-sparse channels comparing to the adversarial loss

Model	Size	Dataset	Loss	Quant	Ch Sparsity	N	A_1	A_2	A_3
En ₂ ResNet20	0.54M	MNIST	(9)	BR	N/A	99.22%	98.90%	98.90%	99.12%
ResNet44	0.66M	MNIST	TRADES	Float	N/A	99.31%	98.98%	98.91%	99.14%
En ₂ ResNet20	0.54M	MNIST	(9)	Float	N/A	99.21%	99.02%	98.91%	99.14%
En ₂ ResNet20	0.54M	FMNIST	(9)	BR	N/A	91.69%	87.85%	87.22%	89.74%
ResNet44	0.66M	FMNIST	TRADES	Float	N/A	91.37%	88.13%	87.98%	90.12%
En ₂ ResNet20	0.54M	FMNIST	(9)	Float	N/A	92.74%	89.35%	88.68%	91.72%
En ₁ ResNet56	0.85M	Cifar10	(9)	4-bit	33.18%	79.44%	55.71%	47.81%	65.50%
ResNet56	0.85M	Cifar10	TRADES	Float	N/A	78.92%	55.27%	50.40%	59.48%
En ₁ ResNet56	0.85M	Cifar10	(9)	Float	N/A	81.63%	56.80%	50.17%	66.56%
En ₁ ResNet110	1.7M	Cifar100	(9)	4-bit	23.93%	53.08%	30.76%	25.73%	42.54%
ResNet110	1.7M	Cifar100	TRADES	Float	N/A	51.65%	28.23%	25.77%	40.79%
En ₁ ResNet110	1.7M	Cifar100	(9)	Float	N/A	56.63%	32.24%	26.72%	43.99%
En ₂ ResNet56	1.7M	SVHN	(9)	4-bit	49.03%	91.21%	70.91%	57.99%	72.44%
ResNet110	1.7M	SVHN	TRADES	Float	N/A	88.33%	64.80%	56.81%	69.79%
En ₂ ResNet56	1.7M	SVHN	(9)	Float	N/A	93.33%	78.08%	59.11%	75.79%

TABLE VIII: Generalization of quantized models to more datasets. EnResNet with quantized weights and channel sparsity can have similar or even better performance than float TRADES-trained ResNet with the same size. For some datasets, quantized models can perform as good as its float equivalent.

Cifar10, and Cifar100, using models with 4-bit quantization. As in Table VIII, our 4-bit models have better performance than Trades-trained models with the same sizes. However, quantized models on these larger datasets are outperformed by their float equivalents. In another word, efficiency of models are not 'free' when learning large datasets, we have to trade-off between performance and efficiency. Although 4-bit quantization requires higher precision and, as a result, more memories, the highly structured sparsity can compensate the efficiency of models. The 4-bit quantized models of $\text{En}_1\text{ResNet56}$ for Cifar10, $\text{En}_1\text{ResNet110}$ for Cifar 100, and $\text{En}_2\text{ResNet56}$ for SVNH in Table VIII have sizes of 0.58M, 1.43M, and 0.80M respectively if the sparse channels are pruned. Our codes as well as our trained quantized models listed in Table VIII are available at <https://github.com/lzj994/Binary-Quantization>.

VII. CONCLUSION

In this paper, we study the robustness of quantized models. The experimental results suggest that it is totally possible to achieve both efficiency and robustness as quantized models can also do a good job at resisting adversarial attack. Moreover, we discover that high precision quantization can offer sparse DNNs, and a trade-off function can make this sparsity structured. With our integrated approach to balance efficiency and robustness, we find that keeping a model both efficient and robust is promising and worth paying attention to. We hope our study can serve as a benchmark for future studies on this interesting topic.

REFERENCES

- [1] Anish Athalye, Nicholas Carlini, and David Wagner. Obfuscated gradients give a false sense of security: Circumventing defenses to adversarial examples. *arXiv preprint arXiv:1802.00420*, 2018.
- [2] Anish Athalye, Logan Engstrom, Andrew Ilyas, and Kevin Kwok. Synthesizing robust adversarial examples. *arXiv preprint arXiv:1707.07397*, 2017.
- [3] Peter L Bartlett, Michael I Jordan, and Jon D McAuliffe. Convexity, classification, and risk bounds. *Journal of the American Statistical Association*, page 101(473):138–156, 2006.
- [4] Nicholas Carlini and David Wagner. Towards evaluating the robustness of neural networks. In *2017 IEEE Symposium on Security and Privacy (SP)*, pages 39–57. IEEE, 2017.
- [5] T. Chen, Y. Rubanova, J. Bettencourt, and D. Duvenaud. Neural ordinary differential equations. In *Advances in neural information processing systems*, pages 6571–6583, 2018.
- [6] Matthieu Courbariaux, Yoshua Bengio, and Jean-Pierre David. Binaryconnect: Training deep neural networks with binary weights during propagations. In *Advances in neural information processing systems*, pages 3123–3131, 2015.
- [7] Thu Dinh, Bao Wang, Andrea L Bertozzi, Stanley J Osher, and Jack Xin. Sparsity meets robustness: Channel pruning for the feynman-kac formalism principled robust deep neural nets. *arXiv preprint arXiv:2003.00631*, 2020.
- [8] Yinpeng Dong, Qi-An Fu, Xiao Yang, Tianyu Pang, Hang Su, Zihao Xiao, and Jun Zhu. Benchmarking adversarial robustness on image classification. In *IEEE/CVF Conference on Computer Vision and Pattern Recognition*, 2020.
- [9] Ian J Goodfellow, Jonathon Shlens, and Christian Szegedy. Explaining and harnessing adversarial examples. *arXiv preprint arXiv:1412.6572*, 2014.
- [10] Chuan Guo, Mayank Rana, Moustapha Cisse, and Laurens Van Der Maaten. Countering adversarial images using input transformations. *arXiv preprint arXiv:1711.00117*, 2017.
- [11] Kaiming He, Xiangyu Zhang, Shaoqing Ren, and Jian Sun. Deep residual learning for image recognition. In *Proceedings of the IEEE conference on computer vision and pattern recognition*, pages 770–778, 2016.
- [12] Yihui He, Xiangyu Zhang, and Jian Sun. Channel pruning for accelerating very deep neural networks. In *Proceedings of the IEEE International Conference on Computer Vision*, pages 1389–1397, 2017.
- [13] Alex Krizhevsky et al. Learning multiple layers of features from tiny images. 2009.
- [14] Alexey Kurakin, Ian Goodfellow, and Samy Bengio. Adversarial examples in the physical world. *arXiv preprint arXiv:1607.02533*, 2016.
- [15] Alexey Kurakin, Ian Goodfellow, and Samy Bengio. Adversarial machine learning at scale. *arXiv preprint arXiv:1611.01236*, 2016.
- [16] Hao Li, Soham De, Zheng Xu, Christoph Studer, Hanan Samet, and Tom Goldstein. Training quantized nets: A deeper understanding. In *Advances in Neural Information Processing Systems*, pages 5811–5821, 2017.
- [17] Yandong Li, Lijun Li, Liqiang Wang, Tong Zhang, and Boqing Gong. Nattack: Learning the distributions of adversarial examples for an improved black-box attack on deep neural networks. *arXiv preprint arXiv:1905.00441*, 2019.
- [18] Z. Li and Z. Shi. Deep residual learning and pdes on manifold. *arXiv preprint arXiv:1708.05115*, 2017.
- [19] Ziang Long, Penghang Yin, and Jack Xin. Recurrence of optimum for training weight and activation quantized networks. *arXiv preprint arXiv:2012.05529*, 2020.
- [20] Aleksander Madry, Aleksandar Makelov, Ludwig Schmidt, Dimitris Tsipras, and Adrian Vladu. Towards deep learning models resistant to adversarial attacks. *arXiv preprint arXiv:1706.06083*, 2017.
- [21] Yuval Netzer, Tao Wang, Adam Coates, Alessandro Bissacco, Bo Wu, and Andrew Y Ng. Reading digits in natural images with unsupervised feature learning. 2011.
- [22] Mohammad Rastegari, Vicente Ordonez, Joseph Redmon, and Ali Farhadi. Xnor-net: Imagenet classification using binary convolutional neural networks. In *European conference on computer vision*, pages 525–542. Springer, 2016.
- [23] Aman Sinha, Hongseok Namkoong, and John Duchi. Certifying some distributional robustness with principled adversarial training. *arXiv preprint arXiv:1710.10571*, 2017.
- [24] Christian Szegedy, Wojciech Zaremba, Ilya Sutskever, Joan Bruna, Dumitru Erhan, Ian Goodfellow, and Rob Fergus. Intriguing properties of neural networks. *arXiv preprint arXiv:1312.6199*, 2013.
- [25] Dimitris Tsipras, Shibani Santurkar, Logan Engstrom, Alexander Turner, and Aleksander Madry. Robustness may be at odds with accuracy. *arXiv preprint arXiv:1805.12152*, 2018.
- [26] B. Wang, X. Luo, Z. Li, W. Zhu, Z. Shi, and S. Osher. Deep neural nets with interpolating function as output activation. In *Advances in Neural Information Processing Systems*, pages 743–753, 2018.
- [27] Bao Wang, Zuqiang Shi, and Stanley Osher. Resnets ensemble via the feynman-kac formalism to improve natural and robust accuracies. In *Advances in Neural Information Processing Systems*, pages 1655–1665, 2019.
- [28] Yisen Wang, Xingjun Ma, James Bailey, Jinfeng Yi, Bowen Zhou, and Quanquan Gu. On the convergence and robustness of adversarial training. In *International Conference on Machine Learning*, pages 6586–6595, 2019.
- [29] Han Xiao, Kashif Rasul, and Roland Vollgraf. Fashion-mnist: a novel image dataset for benchmarking machine learning algorithms. *arXiv preprint arXiv:1708.07747*, 2017.
- [30] Penghang Yin, Shuai Zhang, Jiancheng Lyu, Stanley Osher, Yingyong Qi, and Jack Xin. Binaryrelax: A relaxation approach for training deep neural networks with quantized weights. *SIAM Journal on Imaging Sciences*, 11(4):2205–2223, 2018.
- [31] Hongyang Zhang, Yaodong Yu, Jiantao Jiao, Eric P Xing, Laurent El Ghaoui, and Michael I Jordan. Theoretically principled trade-off between robustness and accuracy. *International Conference on Machine Learning*, 2019.
- [32] Zhuangwei Zhuang, Minghui Tan, Bohan Zhuang, Jing Liu, Yong Guo, Qingyao Wu, Junzhou Huang, and Jinhui Zhu. Discrimination-aware channel pruning for deep neural networks. In *Advances in Neural Information Processing Systems*, pages 875–886, 2018.